Available online at www.sciencedirect.com
SCIENCE DIRECT
Sensors and Actuators A 129 (2006) 1–5
SENSORS AND ACTUATORS A PHYSICAL
www.elsevier.com/locate/sna

Laser-pumped cesium magnetometers for high-resolution medical and fundamental research

S. Groeger [a], G. Bison [a,*], P.E. Knowles [a], R. Wynands [b], A. Weis [a]

[a] *University of Fribourg, Physics Department, 1700 Fribourg, Switzerland*
[b] *PTB 4.41, 38116 Braunschweig, Germany*

Received 4 July 2004; received in revised form 26 November 2004; accepted 19 September 2005
Available online 20 December 2005

Abstract

Laser-pumped cesium magnetometers allow highly sensitive magnetometry at room temperature. We report on applications of that technique in biomagnetic diagnostics and in a neutron electric dipole moment (nEDM) experiment. In the biomagnetic application the magnetic field from the beating human heart is detected using a gradiometer, which reaches an intrinsic sensitivity of 80 fT/Hz$^{1/2}$. The device can record time-resolved magnetic field maps above the human body surface with a spatial resolution of 4 cm and its performance is comparable to commercial devices based on the SQUID technique. In the nEDM experiment laser-pumped cesium magnetometers are used to measure and stabilize a dc magnetic field at a level of 10^{-7}. Those devices reach an intrinsic sensitivity of about 14 fT/Hz$^{1/2}$ with a measurement bandwidth of 1 kHz. The general principle of operation and specific results are presented.

Keywords: Optical magnetometry; Spin physics; Cardiomagnetometry; Magnetocardiogram; Electric dipole moment

1. Introduction

In many areas of fundamental and applied science the sensitive detection of weak magnetic fields and small field fluctuations is of great importance. Experiments looking for small violations of discrete symmetries in atoms and particles (such as the neutron) require precise control of the magnetic field. In past experiments looking for an electric dipole moment (EDM) of the neutron magnetic fields were measured by optically pumped alkali magnetometers, which monitored the field at several positions outside the neutron experimental volume [1], or by optically pumped ^{199}Hg, which acted as a comagnetometer in the volume occupied by the neutrons [2]. The precession frequency of ^{199}Hg in a 1 μT field is about 8 Hz, and the time resolution for that magnetometer type is very low. In contrast to this, optically pumped cesium magnetometers offer the possibility for fast real-time field measurements with more than 100 times larger bandwidth due to the larger gyromagnetic ratio and variable spatial resolution. That property is very important in our second area of interest, the measurement of magnetic fields produced by biological organisms, which contain valuable information on the underlying physiological processes and associated pathologies [3]. Currently superconducting quantum interference devices (SQUID) cooled far below room temperature were required to measure those weak biomagnetic signals. The requirements for a useful magnetic field sensor for biomagnetic detection are, besides an ultra-high sensitivity, a time resolution in the millisecond range and a spatial resolution on the cm-scale, conditions which both can be met by optically pumped cesium magnetometers.

2. Optically pumped magnetometers

The principle of optically pumped magnetometers (OPM) using alkali vapors was developed in the second half of the last century using discharge lamps as light sources [4]. Since then a steady development in electronics and in semiconductor laser technology has allowed the development of devices with sensitivities of a few fT/Hz$^{1/2}$ [5] or less [6]. Here we introduce the OPM technique as employed by our group.

The scheme of an OPM is shown in Fig. 1. A circularly polarized light beam (from a tunable extended-cavity diode laser)

* Corresponding author. Tel.: +41 26 300 9031; fax: +41 26 300 9631.
E-mail address: georg.bison@unifr.ch (G. Bison).

0924-4247/$ – see front matter © 2005 Elsevier B.V. All rights reserved.
doi:10.1016/j.sna.2005.09.036

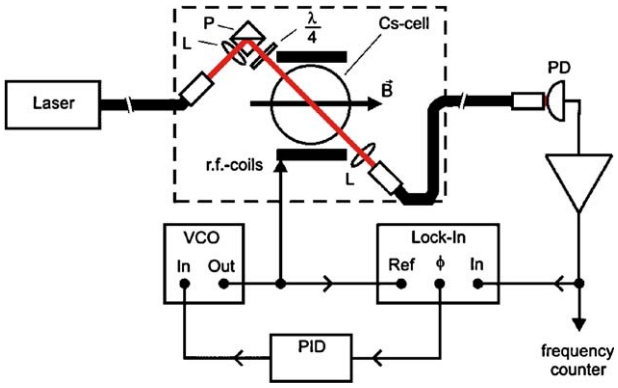

Fig. 1. Schematic setup of the phase-stabilized magnetometer. The dashed box indicates the sensor. L: lens, P: polarizing beam splitter, λ/4: quarter-wave plate, PD: photodiode, VCO: voltage-controlled oscillator, PID: feedback amplifier. The stabilization system for the laser frequency is not shown.

traverses a vapor of cesium atoms. The light frequency is tuned to the $(6^2S_{1/2})\ F=4 \rightarrow (6^2P_{1/2})\ F=3$ hyperfine transition of the D_1 line at 894 nm, and the laser frequency is locked by a dichroic atomic vapor laser lock (DAVLL) [7], which provides a continuous stable operation over weeks. Due to optical pumping [8] the equilibrium populations of the Zeeman substrates in the sample are changed and a macroscopic net magnetization is induced along the light propagation direction. In an external magnetic field B_0, the magnetization processes around the field direction with the Larmor frequency $\omega_L = 2\pi\gamma B_0$, where $\gamma = 3.5$ Hz/nT is the gyromagnetic ratio of Cs. The measurement of the magnetic field is thus transferred to a frequency measurement. In the geometry used here, the so-called M_x configuration, B_0 subtends an angle of 45° with the light propagation direction. The precession is resonantly driven by a transverse radiofrequency (r.f.) field $B_1(t)$ oscillating at the frequency ω_{rf}, which leads to a periodically changing projection of the magnetization on the light direction at the frequency ω_{rf}. This results in a modulation of the optical absorption coefficient and thus of the light power transmitted through the cesium sample. That modulation can be monitored by detecting either its in-phase component, its quadrature component, or its phase with respect to the oscillating r.f. field. All three signals show a resonant behavior when ω_{rf} is scanned across ω_L; in particular the phase on resonance is −90°.

The magnetometer is operated by actively stabilizing ω_{rf}, generated by a voltage-controlled oscillator (VCO), to the Larmor frequency by an electronic feedback loop, and the magnetometer signal is obtained by measuring the radiofrequency ω_{rf} in the locked mode. Both the in-phase and the phase signals have a dispersive dependence on the detuning which provide an error signal for the servo loop in order to lock the phase to −90°. The magnetometer is then said to be operated in the phase-stabilized mode. The magnetic field range of the magnetometer is limited by the frequency range of the VCO, whereas the response bandwidth to magnetic field changes depends on the loop filters. Note that in principle the maximum bandwidth of an optically pumped magnetometer is given by the Larmor frequency of the atoms.

The resolution of a magnetic field measurement depends on the noise equivalent magnetic field (NEM), which is the magnetic field change δB that induces a detector signal equivalent to the signal noise:

$$\delta B = \delta B_{int} + \delta B_{ext}, \tag{1}$$

where δB_{int} is the noise inherent to the magnetometer and δB_{ext} are magnetic field fluctuations. The NEM δB_{int} can be determined directly only from the noise of a magnetic field measurement in a perfectly stable field ($\delta B_{ext} = 0$). In that case the Fourier spectrum of the OPM signal would show a single peak at the Larmor frequency (carrier) superposed on a noise background corresponding to the magnetometer noise. Magnetic field fluctuations, as well as, e.g., laser power fluctuations or electronic noise, will appear as sidebands of the carrier in the Fourier spectrum. Eq. (1) can thus be written as:

$$\delta B = \frac{1}{\gamma}\frac{\Delta\nu}{S/N}, \tag{2}$$

where $\Delta\nu$ is the half linewidth of the resonance and S/N the signal-to-noise ratio of the modulation signal at the Larmor frequency. The noise level $N\left(=\sqrt{N_{SN}^2 + N_{OPM}^2 + N_{ext}^2}\right)$, measured in a bandwidth f_{bw}, consists of the shot noise N_{SN} originating from the current noise $\Delta I\left(=\sqrt{2e\, I_{pc}\, f_{bw}}\right)$ of the photodiode current I_{pc}, the noise inherent to the magnetometer proper, N_{OPM}, and external field fluctuations which can be parametrized as N_{ext}. In Fig. 2 a typical FFT spectrum of an OPM inside a three-layer magnetic shield is shown. The peak at the Larmor frequency is superposed on a broad pedestal that stems from external magnetic field fluctuations. The sidebands at 50 Hz appear due to an incomplete shielding of the power-line field. The white noise floor in the far wings of the spectrum corresponds to $N_{int}\left(=\sqrt{N_{SN}^2 + N_{OPM}^2}\right)$ at the carrier frequency and allows us to infer the inherent magnetometer NEM δB_{int}.

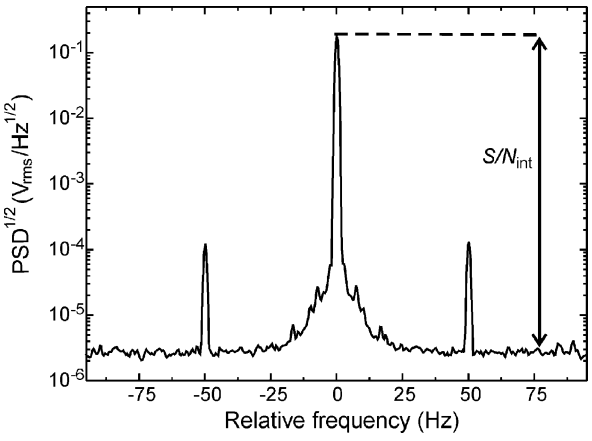

Fig. 2. Square root of the power spectral density (PSD) of the magnetometer output frequency relative to the Larmor frequency of $\nu_L = 7032$ Hz (averaged 20 times). The spectrum was measured with a 1 Hz resolution bandwidth. The signal-to-noise ratio S/N_{int} is approximately 66,000. The sidebands are due to imperfectly shielded magnetic field components oscillating at the 50-Hz power-line frequency.